2013 IEEE 10th International Symposium on Biomedical Imaging:
From Nano to Macro
San Francisco, CA, USA, April 7-11, 2013

SURE-BASED PARAMETER SELECTION FOR PARALLEL MRI RECONSTRUCTION USING GRAPPA AND SPARSITY

Daniel S. Weller[⋆] *Sathish Ramani*[⋆] *Jon-Fredrik Nielsen*[†] *Jeffrey A. Fessler*[⋆,†]

[⋆]EECS Department, University of Michigan, Ann Arbor, MI, USA
[†]BME Department, University of Michigan, Ann Arbor, MI, USA

ABSTRACT

New methods have been developed for parallel MRI reconstruction combining GRAPPA and sparsity. One impediment to the practical application of such methods is selecting a regularization parameter that acceptably balances the contributions of GRAPPA and sparsity. We propose a broadly applicable Monte-Carlo-based approximation to Stein's unbiased risk estimate (SURE) for a suitable weighted mean-squared error (WMSE) metric. Applying this approximation to predict the WMSE-optimal tuning parameter for sparsity-based reconstruction, we are able to tune our parameter to achieve nearly MSE-optimal performance. In our simulations, we vary the noise level in the simulated data and use our Monte-Carlo method to tune the reconstruction to the noise level automatically.

***Index Terms*—** Parallel imaging, MRI, regularization parameter selection, sparsity, Stein's unbiased risk estimate, Monte-Carlo methods.

1. INTRODUCTION

GRAPPA [1] is a popular reconstruction method for parallel imaging that does not require explicit knowledge of the coil sensitivities and, in the uniformly spaced undersampling case, yields a direct expression for the missing k-space. Sparsity has been successfully applied in many ways to improve MRI reconstruction [2], but as with any regularization method, parameter selection hinders widespread adoption. The Denoising Sparse Images from GRAPPA using the Nullspace (DESIGN) method [3] employs a regularization parameter to balance fidelity to the GRAPPA reconstruction with transform-domain joint sparsity of the reconstructed coil images. By approximating the mean-squared error (MSE), Stein's unbiased risk estimate (SURE) [4] provides a reasonable criterion for automatic parameter selection.

We propose a Monte-Carlo-based technique geared to parallel MRI with complex-valued k-space that allows us to estimate SURE for each of several candidate tuning parameter values using two evaluations of the reconstruction method per parameter choice. As opposed to traditional Monte-Carlo estimation, our approach does not require averaging multiple realizations because the thousands of k-space points a typical data set contains effectively reduces the variance of our estimate. Our derivation follows the approach for single-coil MRI [5]. We illustrate the benefits of Monte-Carlo-based SURE estimation using DESIGN because it (a) employs GRAPPA in the reconstruction and does not rely on coil sensitivities and (b) preserves the acquired k-space data in the reconstruction. In this paper, we demonstrate that for simulated brain images, the Monte-Carlo-based SURE approximation yields a tuning parameter for DESIGN that performs nearly MSE-optimally, without prior knowledge of the true signal.

We begin by describing our data model and our notation for GRAPPA reconstruction. Then, we derive our weighted error measure WMSE for GRAPPA parallel imaging from the MSE and our SURE-based estimate WSURE for this WMSE. We explain our Monte-Carlo-based scheme for estimating the WSURE using just two evaluations of the reconstruction function, and apply it to automatic parameter tuning for DESIGN. We conclude with simulations employing our method with simulated brain data depicting nearly MSE-optimal performance over a range of noise levels.

2. DATA MODEL

Consider the vector of unknown noise-free samples $\mathbf{x} \in \mathbb{C}^{NL}$ of N k-space locations using L coils. We acquire $M \leq N$ samples from all the coils, yielding k-space observations $\mathbf{y} \in \mathbb{C}^{ML}$ according to

$$\mathbf{y} = \mathbf{M}\,\mathbf{x} + \boldsymbol{\xi}, \tag{1}$$

where the mask $\mathbf{M} = \mathbf{I}_L \otimes \mathbf{T}$, $\mathbf{T}$ is a $M \times N$ down-sampled identity matrix representing undersampling of k-space, and we ignore field inhomogeneities and relaxation effects. The above model applies equally well to uniform and arbitrary Cartesian sampling. These observations are corrupted by complex-valued Gaussian noise $\boldsymbol{\xi} \in \mathbb{C}^{ML}$ such that $\mathcal{E}_{\boldsymbol{\xi}}\{\boldsymbol{\xi}\} = \mathbf{0}$, $\mathcal{E}_{\boldsymbol{\xi}}\{\boldsymbol{\xi}\boldsymbol{\xi}^\top\} = \mathbf{0}$, and $\mathcal{E}_{\boldsymbol{\xi}}\{\boldsymbol{\xi}\boldsymbol{\xi}'\} = \boldsymbol{\Omega} \in \mathbb{C}^{ML \times ML}$, where $\boldsymbol{\Omega} \succ 0$ is a Hermitian-symmetric positive definite matrix, and $(\cdot)'$ and $(\cdot)^\top$ are the conjugated and non-conjugated transposes, respectively, of a (complex-valued) vector or matrix. The probability density function of $\boldsymbol{\xi}$ is given by

$$g(\boldsymbol{\xi}) = K \exp\left(-\boldsymbol{\xi}'\boldsymbol{\Omega}^{-1}\boldsymbol{\xi}\right), \tag{2}$$

where K is a normalization constant.

3. GRAPPA AS A LINEAR OPERATOR

GRAPPA reconstructs missing k-space locations through a linear transformation $\mathbf{G} \in \mathbb{C}^{NL \times ML}$ of the observed data $\mathbf{y}$, given by

$$\mathbf{G} \triangleq \mathbf{M}' + \widetilde{\mathbf{M}}'\boldsymbol{\mathcal{G}}, \tag{3}$$

where $\boldsymbol{\mathcal{G}} \in \mathbb{C}^{(N-M)L \times ML}$ acts on $\mathbf{y}$ to fill in the missing k-space locations specified by $\widetilde{\mathbf{M}} = \mathbf{I}_L \otimes \widetilde{\mathbf{T}}$, and $\widetilde{\mathbf{T}}$ is a $(N-M) \times N$ subsampling matrix that selects all the rows from $\mathbf{I}_N$ that are not already in $\mathbf{T}$. It is easy to see that $\mathbf{M}\mathbf{M}' = \mathbf{I}_{ML}$, $\widetilde{\mathbf{M}}\widetilde{\mathbf{M}}' = \mathbf{I}_{(N-M)L}$, and $\widetilde{\mathbf{M}}\mathbf{M}' = \mathbf{M}\widetilde{\mathbf{M}}' = \mathbf{0}$. While $\boldsymbol{\mathcal{G}}$ is calibrated from noisy training data, we treat $\boldsymbol{\mathcal{G}}$ as deterministic and fixed (see Lemma 1).

Funding acknowledgments: NIH F32 EB015914 and NIH/NCI P01 CA87634.

4. QUADRATIC ERROR MEASURES

In the sequel, we are interested in an estimator $\mathbf{f}_{\boldsymbol{\gamma}}(\mathbf{y})$ with tunable parameters $\boldsymbol{\gamma} \in \mathbb{R}^n$ that yields an estimate of the full multi-coil k-space $\mathbf{x}$. MSE-type measures are often used to quantify image quality in reconstruction problems. To minimize MSE, one would adjust $\boldsymbol{\gamma}$ so as to minimize

$$\mathrm{MSE}(\boldsymbol{\gamma}) \triangleq \|\mathbf{x} - \mathbf{f}_{\boldsymbol{\gamma}}(\mathbf{y})\|_2^2. \tag{4}$$

However, $\mathrm{MSE}(\boldsymbol{\gamma})$ is neither accessible in practice nor can be estimated from $\mathbf{y}$ due to rank-deficiency of $\mathbf{M}$. To get around this limitation, we assert that $\mathbf{GMx} \approx \mathbf{x}$ in the noise-free case (i.e., GRAPPA does a good job filling the missing k-space). Since GRAPPA preserves the acquired data $\mathbf{y}$ exactly, we compute the WMSE over only the remaining (missing) data:

$$\mathrm{WMSE}_{\widetilde{\mathbf{M}}}(\boldsymbol{\gamma}) \triangleq \|\widetilde{\mathbf{M}}(\mathbf{GMx} - \mathbf{f}_{\boldsymbol{\gamma}}(\mathbf{y}))\|_2^2, \tag{5}$$

$$= \|\boldsymbol{\mathcal{G}}\mathbf{Mx} - \widetilde{\mathbf{M}}\mathbf{f}_{\boldsymbol{\gamma}}(\mathbf{y})\|_2^2 \tag{6}$$

Since DESIGN also preserves the acquired data, we write

$$\mathbf{f}_{\boldsymbol{\gamma}}(\mathbf{y}) = \mathbf{M}'\mathbf{y} + \widetilde{\mathbf{M}}'\mathbf{g}_{\boldsymbol{\gamma}}(\mathbf{y}), \tag{7}$$

where $\mathbf{g}_{\boldsymbol{\gamma}} : \mathbb{C}^{ML} \to \mathbb{C}^{(N-M)L}$ reconstructs the missing k-space. For such data-preserving $\mathbf{f}_{\boldsymbol{\gamma}}$, $\mathrm{WMSE}_{\widetilde{\mathbf{M}}}(\boldsymbol{\gamma})$ reduces to

$$\mathrm{WMSE}_{\widetilde{\mathbf{M}}}(\boldsymbol{\gamma}) = \|\boldsymbol{\mathcal{G}}\mathbf{Mx} - \mathbf{g}_{\boldsymbol{\gamma}}(\mathbf{y})\|_2^2. \tag{8}$$

In this paper, we will focus on $\mathbf{f}_{\boldsymbol{\gamma}}$ that is of this form and use $\mathrm{WMSE}_{\widetilde{\mathbf{M}}}(\boldsymbol{\gamma})$. However, our argument can be extended to other quadratic error measures including other weighted $\mathrm{MSE}(\boldsymbol{\gamma})$.

Expanding the quadratic and making the substitution $\mathbf{Mx} = \mathbf{y} - \boldsymbol{\xi}$,

$$\begin{aligned}\mathrm{WMSE}_{\widetilde{\mathbf{M}}}(\boldsymbol{\gamma}) = \|\mathbf{g}_{\boldsymbol{\gamma}}(\mathbf{y})\|_2^2 - 2\mathcal{R}\{\mathbf{y}'\boldsymbol{\mathcal{G}}'\mathbf{g}_{\boldsymbol{\gamma}}(\mathbf{y})\} + C \\ + 2\mathcal{R}\{\boldsymbol{\xi}'\boldsymbol{\mathcal{G}}'\mathbf{g}_{\boldsymbol{\gamma}}(\mathbf{y})\},\end{aligned} \tag{9}$$

where $\mathcal{R}\{\cdot\}$ denotes the real part of a complex number and $C \triangleq \|\boldsymbol{\mathcal{G}}\mathbf{Mx}\|_2^2$ is an irrelevant constant that does not depend on $\boldsymbol{\gamma}$. The only other term that is not accessible in (9) is $\boldsymbol{\xi}'\boldsymbol{\mathcal{G}}'\mathbf{g}_{\boldsymbol{\gamma}}(\mathbf{y})$. We use Stein's principle to estimate this term in the sequel.

5. USING STEIN'S LEMMA TO ESTIMATE $\mathrm{WMSE}_{\widetilde{\mathbf{M}}}(\boldsymbol{\gamma})$

It is easy to see that $g(\boldsymbol{\xi})$ in (2) satisfies the following:

$$\nabla_{\boldsymbol{\xi}} g(\boldsymbol{\xi}) = -g(\boldsymbol{\xi})\,\boldsymbol{\xi}'\boldsymbol{\Omega}^{-1}, \tag{10}$$

where $\nabla_{\boldsymbol{\xi}} \triangleq \frac{1}{2}(\nabla_{\boldsymbol{\xi}_{\mathcal{R}}} - \iota\nabla_{\boldsymbol{\xi}_{\mathcal{I}}})$ and $\nabla_{\boldsymbol{\xi}_{\mathcal{R}}}, \nabla_{\boldsymbol{\xi}_{\mathcal{I}}}$ are $1 \times ML$ gradient operators with respect to the real, $\boldsymbol{\xi}_{\mathcal{R}}$, and imaginary, $\boldsymbol{\xi}_{\mathcal{I}}$, parts of $\boldsymbol{\xi}$, respectively. This identity can be used to estimate $\mathcal{E}_{\boldsymbol{\xi}}\{\boldsymbol{\xi}'\boldsymbol{\mathcal{G}}'\mathbf{g}_{\boldsymbol{\gamma}}(\mathbf{y})\}$ as follows.

Lemma 1. *Let $\mathbf{g}_{\boldsymbol{\gamma}} : \mathbb{C}^{ML} \to \mathbb{C}^{(N-M)L}$ be individually analytic with respect to real and imaginary parts of its argument (in the weak sense of distributions). Then, as long as the deterministic matrix $\boldsymbol{\mathcal{G}}$ satisfies $\mathcal{E}_{\boldsymbol{\xi}}\{|[\boldsymbol{\mathcal{G}}'\mathbf{g}_{\boldsymbol{\gamma}}(\mathbf{y})]_m|\} < \infty$, $m = 1, \ldots, ML$, we have*

$$\mathcal{E}_{\boldsymbol{\xi}}\{\boldsymbol{\xi}'\boldsymbol{\mathcal{G}}'\mathbf{g}_{\boldsymbol{\gamma}}(\mathbf{y})\} = \mathcal{E}_{\boldsymbol{\xi}}\left\{\mathrm{tr}\{\boldsymbol{\Omega}\boldsymbol{\mathcal{G}}'\mathbf{J}_{\mathbf{g}_{\boldsymbol{\gamma}}}(\mathbf{y})\}\right\}, \tag{11}$$

where $\mathbf{J}_{\mathbf{g}_{\boldsymbol{\gamma}}}(\mathbf{y})$ is the Jacobian matrix of partial derivatives of $\mathbf{g}_{\boldsymbol{\gamma}}$ w.r.t. components of $\mathbf{y}$ and is defined via its elements as

$$[\mathbf{J}_{\mathbf{g}_{\boldsymbol{\gamma}}}(\mathbf{y})]_{qp} \triangleq \frac{1}{2}\left(\frac{\partial[\mathbf{g}_{\boldsymbol{\gamma}}(\mathbf{y})]_q}{\partial y_{\mathcal{R}p}} - \iota\frac{\partial[\mathbf{g}_{\boldsymbol{\gamma}}(\mathbf{y})]_q}{\partial y_{\mathcal{I}p}}\right). \tag{12}$$

Proof. The proof for a general noise covariance $\boldsymbol{\Omega}$ is similar to that for $\boldsymbol{\Omega} = \mathbf{I}$ in [5]. □

We now use (11) to show that

$$\begin{aligned}\mathrm{WSURE}(\boldsymbol{\gamma}) \triangleq \|\mathbf{g}_{\boldsymbol{\gamma}}(\mathbf{y})\|_2^2 - 2\mathcal{R}\{\mathbf{y}'\boldsymbol{\mathcal{G}}'\mathbf{g}_{\boldsymbol{\gamma}}(\mathbf{y})\} + C \\ + 2\,\mathcal{R}\{\mathrm{tr}\{\boldsymbol{\Omega}\boldsymbol{\mathcal{G}}'\mathbf{J}_{\mathbf{g}_{\boldsymbol{\gamma}}}(\mathbf{y})\}\}.\end{aligned} \tag{13}$$

is an unbiased estimate of $\mathrm{WMSE}_{\widetilde{\mathbf{M}}}(\boldsymbol{\gamma})$.

Theorem 1. *Let $\mathbf{g}_{\boldsymbol{\gamma}}(\mathbf{y})$ and $\boldsymbol{\mathcal{G}}$ satisfy the hypotheses of Lemma 1. Then $\mathcal{E}_{\boldsymbol{\xi}}\{\mathrm{WSURE}(\boldsymbol{\gamma})\} = \mathcal{E}_{\boldsymbol{\xi}}\{\mathrm{WMSE}_{\widetilde{\mathbf{M}}}(\boldsymbol{\gamma})\}$.*

The proof is straightforward and uses Lemma 1 to estimate $\boldsymbol{\xi}'\boldsymbol{\mathcal{G}}'\mathbf{g}_{\boldsymbol{\gamma}}(\mathbf{y})$ in (9). In practice, one can ignore the irrelevant constant C in (13) and the expectation $\mathcal{E}$ is dropped. WSURE is independent of $\mathbf{x}$ and depends only on $\mathbf{y}$, $\mathbf{g}_{\boldsymbol{\gamma}}$ via $\mathrm{tr}\{\boldsymbol{\Omega}\boldsymbol{\mathcal{G}}'\mathbf{J}_{\mathbf{g}_{\boldsymbol{\gamma}}}(\mathbf{y})\}$ and the noise covariance matrix $\boldsymbol{\Omega}$.

While $\mathbf{J}_{\mathbf{g}_{\boldsymbol{\gamma}}}(\mathbf{y})$ in (13) may be evaluated (recursively) analytically for a (iterative) $\mathbf{g}_{\boldsymbol{\gamma}}$ (as done in [5]), we propose a Monte-Carlo scheme for numerically estimating $\mathrm{tr}\{\boldsymbol{\Omega}\boldsymbol{\mathcal{G}}'\mathbf{J}_{\mathbf{g}_{\boldsymbol{\gamma}}}(\mathbf{y})\}$ in WSURE (13). The proposed approach does not require knowledge of the internal working of $\mathbf{g}_{\boldsymbol{\gamma}}$ as we shall see next; this advantage makes it readily applicable to a wide variety of $\mathbf{g}_{\boldsymbol{\gamma}}$ (admissible by Lemma 1).

6. MONTE-CARLO ESTIMATION OF $\mathrm{WSURE}(\boldsymbol{\gamma})$

Next, we extend the Monte-Carlo method of [6] to complex $\mathbf{g}_{\boldsymbol{\gamma}}$.

Theorem 2. *Let $\mathbf{g}_{\boldsymbol{\gamma}}$ admit a second-order Taylor expansion in addition to satisfying the hypotheses in Lemma 1. Consider the random vector*

$$\boldsymbol{\varrho}(\varepsilon) \triangleq \frac{\mathbf{g}_{\boldsymbol{\gamma}}(\mathbf{y} + \varepsilon\mathbf{b}) - \mathbf{g}_{\boldsymbol{\gamma}}(\mathbf{y})}{\varepsilon}, \tag{14}$$

where $\mathbf{b} \in \mathbb{C}^{ML}$ is an i.i.d. random vector independent of $\mathbf{y}$ such that $\mathcal{E}_{\mathbf{b}}\{\mathbf{b}\} = \mathbf{0}$, $\mathcal{E}_{\mathbf{b}}\{\mathbf{b}\mathbf{b}^\top\} = \mathbf{0}$, $\mathcal{E}_{\mathbf{b}}\{\mathbf{b}\mathbf{b}'\} = \mathbf{I}_{ML}$. Then

$$\mathrm{tr}\{\boldsymbol{\Omega}\boldsymbol{\mathcal{G}}'\mathbf{J}_{\mathbf{g}_{\boldsymbol{\gamma}}}(\mathbf{y})\} = \lim_{\varepsilon\to 0}\mathcal{E}_{\mathbf{b}}\{\mathbf{b}'\boldsymbol{\Omega}\boldsymbol{\mathcal{G}}'\,\boldsymbol{\varrho}(\varepsilon)\}. \tag{15}$$

The proof involves manipulating the terms of a second order Taylor expansion of $\mathbf{g}_{\boldsymbol{\gamma}}(\mathbf{y})$ using the commutativity of the trace operator, and the second-order statistics of $\mathbf{b}$.

Remark 1. *In practice, $\mathbf{g}_{\boldsymbol{\gamma}}$ may not always admit a second-order Taylor expansion as required in Theorem 2. In such cases, it is possible to extend the above result (15) in the weak sense of distributions similar to that documented in Theorem 2 of [6].*

Remark 2. *In practice, the limit in (15) cannot be resolved analytically, so we use the approximation*

$$\mathrm{tr}\{\boldsymbol{\Omega}\boldsymbol{\mathcal{G}}'\mathbf{J}_{\mathbf{g}_{\boldsymbol{\gamma}}}(\mathbf{y})\} \approx \mathbf{b}'\boldsymbol{\Omega}\boldsymbol{\mathcal{G}}'\,\boldsymbol{\varrho}(\varepsilon). \tag{16}$$

for sufficiently small $\varepsilon \approx 0$ and one realization of a complex-valued $\mathbf{b}$, where we have dropped the expectation $\mathcal{E}_{\mathbf{b}}$ w.r.t. $\mathbf{b}$ in (16).

Remark 3. *Computing $\mathrm{tr}\{\boldsymbol{\Omega}\boldsymbol{\mathcal{G}}'\mathbf{J}_{\mathbf{g}_{\boldsymbol{\gamma}}}(\mathbf{y})\}$ (15) only requires the response of $\mathbf{g}_{\boldsymbol{\gamma}}$ to $\mathbf{y}$ and $\mathbf{y} + \varepsilon\mathbf{b}$ for a complex-valued $\mathbf{b}$ and does not need the knowledge of internal workings of $\mathbf{g}_{\boldsymbol{\gamma}}$, so (16) is very flexible in its applicability.*

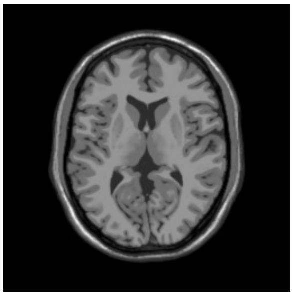

Fig. 1. The sum-of-squares combined ground-truth (no noise).

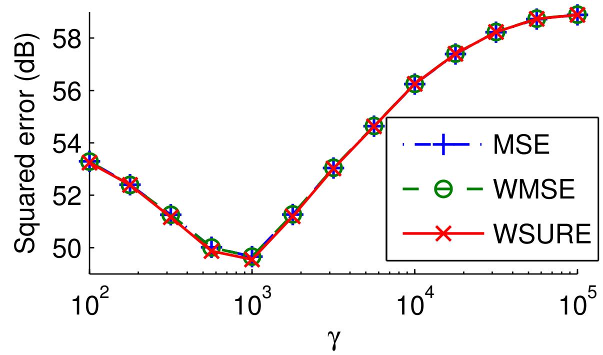

Fig. 2. True MSE, WMSE, and estimated WSURE values closely match across a wide range of γ's.

7. APPLICATION TO DESIGN

DESIGN denoising [3] jointly minimizes a least-squares term promoting fidelity to the GRAPPA-reconstructed k-space and a $\ell_{1,2}$ hybrid norm promoting joint sparsity in an appropriate sparse transform domain of the parallel-receive coil images. In particular, we optimize over the missing data $\mathbf{v} \in \mathbb{C}^{(N-M)L}$:

$$\mathbf{g}_{\boldsymbol{\gamma}}(\mathbf{y}) = \arg\min_{\mathbf{v}} \frac{1}{2}\|\mathbf{v} - \boldsymbol{\mathcal{G}}\mathbf{y}\|^2_{\boldsymbol{\Omega}_{\mathbf{G}}} + \gamma\|\boldsymbol{\Psi}\mathcal{F}^{-1}(\widetilde{\mathbf{M}}'\mathbf{v} + \mathbf{M}'\mathbf{y})\|_{1,2}. \tag{17}$$

The least-squares term is normalized using a block-diagonal approximation to the GRAPPA-amplified noise covariance $\boldsymbol{\Omega}_{\mathbf{G}} = \boldsymbol{\mathcal{G}}\boldsymbol{\Omega}\boldsymbol{\mathcal{G}}'$, which is described in [7]. We solve (17) efficiently using Split-Bregman iteration [8], introducing the auxiliary variable $\mathbf{w} = \boldsymbol{\Psi}\mathcal{F}^{-1}(\widetilde{\mathbf{M}}'\mathbf{v} + \mathbf{M}'\mathbf{y})$. We ran ten iterations of the Split-Bregman algorithm. A four-level bi-orthogonal '9-7' discrete wavelet transform was used to sparsify the coil images.

For Monte-Carlo SURE, complex noise $\mathbf{b}$ was generated with iid Bernoulli real and imaginary parts (satisfying the requirements of Theorem 2), and ε was chosen to be 10^{-3}. Each WSURE estimate uses one realization of complex noise $\mathbf{b}$; only two runs of the DESIGN problem (17) per candidate γ are needed to generate a WSURE estimate. We calculate $\mathbf{b}'\boldsymbol{\Omega}\boldsymbol{\mathcal{G}}'$ once and store it for all γ's.

A 256×256-pixel axial slice of an 1.0 mm isotropic T_1-weighted normal brain was obtained from the BrainWeb database (http://www.bic.mni.mcgill.ca/brainweb/) [9], and this data set was combined with a simulated eight-channel circular array coil and undersampled by two in each direction in k-space using MATLAB. Complex Gaussian noise was added to the samples, and a 24×24 block in the center of k-space was retained to be used as GRAPPA calibration data. Figure 1 shows the fully-sampled reference image without noise.

7.1. Validating WSURE vs. WMSE

To validate our WSURE estimate (13) of the WMSE (5), we plotted the complex Monte-Carlo-based WSURE estimates for a range of γ's logarithmically spaced between 100 and 10^5 against the WMSE's computed using the true acquired k-space values. To facilitate direct comparison of these values, the constant $C = \|\boldsymbol{\mathcal{G}}\mathbf{x}\|^2$ was included in the plot of the WSURE estimate; in practice, this constant is unknown, but it does not affect determining the WSURE-optimal γ.

Over the range of γ's in Figure 2, the WSURE estimate computed using the proposed complex Monte-Carlo SURE is an effective approximation of the true WMSE, and of the true MSE, differing by a maximum of 0.15 dB over a range of 10 dB. We observed similar agreement (not shown) for $\varepsilon = 10^{-4}$ and $\varepsilon = 0.01$.

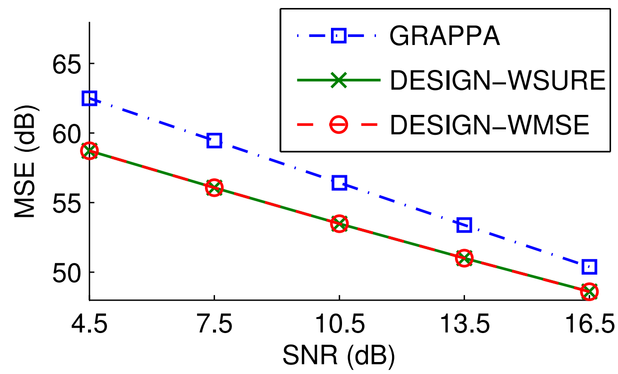

Fig. 3. The WSURE-optimal and WMSE-optimal choices of γ consistently reduce the MSE of the GRAPPA-reconstructed un-acquired k-space by the same amount across a wide range of noise levels.

7.2. Optimal Parameter Tuning for Noise

To determine the MSE-optimal choice of γ over a range of noise levels (SNR from 4.5 to 16.5 dB), we minimized WSURE with respect to γ for the DESIGN method. To avoid local minima, we performed a three-level coarse-to-fine logarithmic parameter sweep on γ. To compare the reconstructions, the MSE based on the true values of the missing k-space was graphed for GRAPPA and DESIGN with the WSURE-optimal γ.

DESIGN using the WSURE-optimal or WMSE-optimal choices of γ improves MSE by up to 4 dB over GRAPPA alone in Figure 3. As shown in Figure 4, this improvement is within 0.014 dB of the optimal reduction in MSE as measured by the ratios of MSEs between DESIGN with WSURE-optimal, WMSE-optimal (based on true values of acquired k-space), and MSE-optimal (based on true values of the missing k-space) choices of γ. In addition, the WMSE-optimal and MSE-optimal reconstructions have nearly the same MSE, validating the assertion that $\boldsymbol{\mathcal{G}}\mathbf{M}\mathbf{x} \approx \widetilde{\mathbf{M}}\mathbf{x}$ underlying our use of WSURE. The sum-of-squares reconstructed and difference images in Figure 5 portray similar improvement in reconstruction quality for DESIGN with WSURE- and WMSE-optimal choices of

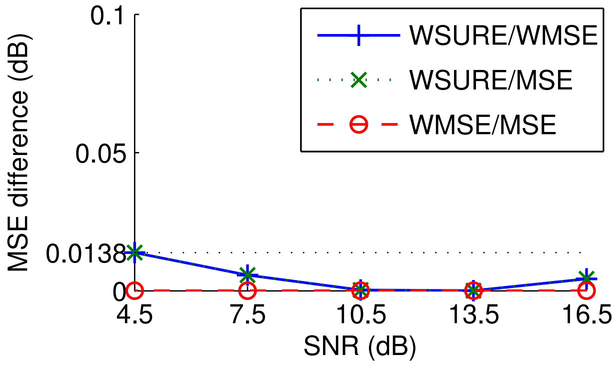

Fig. 4. The MSEs for WSURE-optimal, WMSE-optimal, and MSE-optimal DESIGN are nearly equal to each other over a wide range of noise variances (less than 0.015 dB variation).

γ in the image domain, for the case of 7.5 dB SNR noise. For this noise level, optimizing DESIGN using WSURE involved evaluating 27 choices of γ, each taking 48 seconds on average, for a total run time of 22 minutes. Directly minimizing the WMSE compared 30 choices of γ in 11 minutes, averaging 23 seconds per parameter choice. GRAPPA alone ran in 1.7 seconds.

8. CONCLUSION

We described the WSURE estimator for a weighted-MSE error metric suitable for data-preserving GRAPPA-based parallel imaging reconstruction, proposed a Monte-Carlo-based approximation to the WSURE estimate that requires two evaluations of $\mathbf{g}_{\gamma}(\mathbf{y})$ per candidate parameter choice, and applied the proposed method to find the WSURE-optimal tuning parameter for DESIGN sparsity-based denoising. The ability to achieve nearly MSE-optimal performance justifies using Monte-Carlo-based WSURE estimation for reasonable automatic parameter selection with DESIGN. The proposed Monte-Carlo method generalizes to other parallel-imaging reconstruction algorithms, simplifying the practical application of such algorithms.

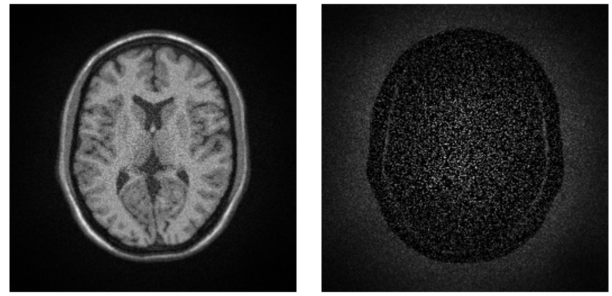

(a) GRAPPA reconstruction.

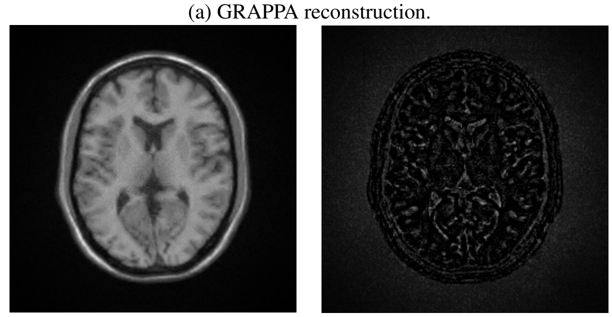

(b) DESIGN (WMSE-optimal γ).

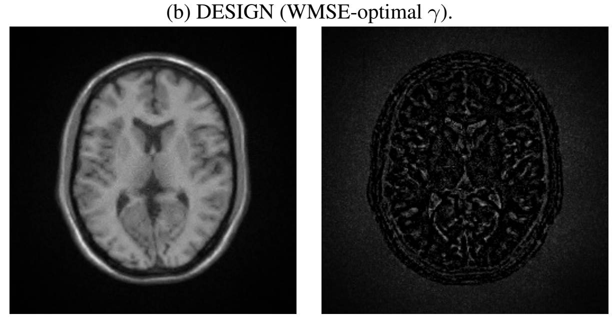

(c) DESIGN (WSURE-optimal γ).

Fig. 5. The GRAPPA reconstruction is denoised within the brain by DESIGN with both the WMSE-optimal and WSURE-optimal γ, leaving behind small residual errors near edges in the original image. The difference images' scales are windowed by a factor of 4.

9. REFERENCES

[1] M. A. Griswold, P. M. Jakob, R. M. Heidemann, M. Nittka, V. Jellus, J. Wang, B. Kiefer, and A. Haase, "Generalized autocalibrating partially parallel acquisitions (GRAPPA)," *Mag. Res. Med.*, vol. 47, no. 6, pp. 1202–10, June 2002.

[2] M. Lustig, D. Donoho, and J. M. Pauly, "Sparse MRI: The application of compressed sensing for rapid MR imaging," *Mag. Res. Med.*, vol. 58, no. 6, pp. 1182–95, Dec. 2007.

[3] D. S. Weller, J. R. Polimeni, L. Grady, L. L. Wald, E. Adalsteinsson, and V. K. Goyal, "Denoising sparse images from GRAPPA using the nullspace method (DESIGN)," *Mag. Res. Med.*, vol. 68, no. 4, pp. 1176–89, Oct. 2012.

[4] C. Stein, "Estimation of the mean of a multivariate normal distribution," *Ann. Stat.*, vol. 9, no. 6, pp. 1135–51, Nov. 1981.

[5] S. Ramani, Z. Liu, J. Rosen, J-F. Nielsen, and J. A. Fessler, "Regularization parameter selection for nonlinear iterative image restoration and MRI reconstruction using GCV and SURE-based methods," *IEEE Trans. Im. Proc.*, vol. 21, no. 8, pp. 3659–72, Aug. 2012.

[6] S. Ramani, T. Blu, and M. Unser, "Monte-Carlo SURE: A black-box optimization of regularization parameters for general denoising algorithms," *IEEE Trans. Im. Proc.*, vol. 17, no. 9, pp. 1540–54, Sept. 2008.

[7] D. S. Weller, J. R. Polimeni, L. Grady, L. L. Wald, E. Adalsteinsson, and V. K. Goyal, "Accelerated parallel magnetic resonance imaging reconstruction using joint estimation with a sparse signal model," in *IEEE Workshop on Statistical Signal Processing*, 2012, pp. 221–4.

[8] T. Goldstein and S. Osher, "The split Bregman method for L1-regularized problems," *SIAM J. Imaging Sci.*, vol. 2, no. 2, pp. 323–43, 2009.

[9] R. K-S. Kwan, A. C. Evans, and G. B. Pike, "MRI simulation-based evaluation of image-processing and classification methods," *IEEE Trans. Med. Imag.*, vol. 18, no. 11, pp. 1085–97, Nov. 1999.